J. Cell. Mol. Med. Vol 20, No 10, 2016 pp. 1872-1888

Selective pressure modulation of synaptic voltage-dependent calcium channels—involvement in HPNS mechanism

Ben Aviner [a, *], Gideon Gradwohl [b], Alice Bliznyuk [a], Yoram Grossman [a]

[a] *Department of Physiology and Neurobiology, Faculty of Health Sciences, Ben-Gurion University of the Negev, Beer Sheva, Israel*
[b] *Department of Physics, Jerusalem College of Technology, Jerusalem, Israel*

Received: November 27, 2015; Accepted: March 21, 2016

Abstract

Exposure to hyperbaric pressure (HP) exceeding 100 msw (1.1 MPa) is known to cause a constellation of motor and cognitive impairments named high-pressure neurological syndrome (HPNS), considered to be the result of synaptic transmission alteration. Long periods of repetitive HP exposure could be an occupational risk for professional deep-sea divers. Previous studies have indicated the modulation of presynaptic Ca^{2+} currents based on synaptic activity modified by HP. We have recently demonstrated that currents in genetically identified cellular voltage-dependent Ca^{2+} channels (VDCCs), $Ca_V1.2$ and $Ca_V3.2$ are selectively affected by HP. This work further elucidates the HPNS mechanism by examining HP effect on Ca^{2+} currents in neuronal VDCCs, $Ca_V2.2$ and $Ca_V2.1$, which are prevalent in presynaptic terminals, expressed in *Xenopus* oocytes. HP augmented the $Ca_V2.2$ current amplitude, much less so in a channel variation containing an additional modulatory subunit, and had almost no effect on the $Ca_V2.1$ currents. HP differentially affected the channels' kinetics. It is, therefore, suggested that HPNS signs and symptoms arise, at least in part, from pressure modulation of various VDCCs.

Keywords: hyperbaric pressure • voltage-dependent calcium channel • high-pressure neurological syndrome

Introduction

Humans, as most terrestrial mammals, are sensitive to hyperbaric pressure (HP). Pressure is a thermodynamic variable affecting the kinetics and steady-state equilibrium of biological processes. Membrane phospholipids fluidity, ion channels, receptors, enzymes and other proteins functions are all potential targets for HP effects [for review, see (1)]. Exposure of humans to HP (usually above 1.0 MPa) causes a constellation of signs and symptoms known as the high-pressure neurological syndrome (HPNS). HPNS is the major problem associated with HP environment, as it occurs due to the effects of pressure *per se* [2, 3]. Divers at depth above 90 msw may exhibit various symptoms, such as dizziness, nausea, tremors, vision and auditory disturbances, decrements in locomotion [4, 5] and cognitive performance [3, 6–9], changes in electroencephalography (EEG) and sleep disorders [10], myoclonus [5], convulsions and a loss of consciousness (for review, see [11]). Alteration in synaptic transmission is a plausible explanation for the HPNS (for review, see [12]). Indeed, HP suppressed synaptic activity in most preparations. This suppression may occur *via* modulation of postsynaptic ionotropic receptors activity [13, 14], decreased AP amplitude [15], slowed kinetics [16, 17], depression of neurotransmitter release [18–21] and modulation of its quantal release mechanism [22–24] and decreased vesicle fusion [13, 19]. Most of these synaptic processes are known to be Ca^{2+} dependent. Earlier studies on crustacean neuromuscular synapses that examined the relationship between $[Ca^{2+}]_o$, excitatory post synaptic potential (EPSC) amplitude and facilitation [25–27] have suggested that pressure depresses Ca^{2+} influx rather than intracellular removal of Ca^{2+}. Further support to this notion was the observations that low $[Ca^{2+}]_o$ partially mimics the effects of HP [20, 27] and high $[Ca^{2+}]_o$ can antagonize to some extent HP depression of current amplitude [15, 25, 28]. In fact, modulation of presynaptic Ca^{2+} currents at HP has been already suggested [15, 29, 30]. We, therefore, postulated that the major mechanism by which HP alters synaptic transmission is the modulation of Ca^{2+} influx into the presynaptic terminals through voltage-dependent Ca^{2+} channels (VDCCs).

Various VDCC subfamilies are known, characterized by their electrophysiological and pharmacological traits: $Ca_V1.1$-4 (L-Types), $Ca_V2.1$ (PQ-type), $Ca_V2.2$ (N-type), $Ca_V2.3$ (R-type) and $Ca_V3.1$-3 (T-types), comprising the α_1, $\alpha_2\delta$, β and γ subunits [31, 32]. The major difference between the channels results from the variation in the α_1 subunit, which holds the ion conducting pore, the voltage sensor, the channel gating section and the known sites of channel regulation by second messengers, drugs and toxins [32]. The $\alpha_2\delta$, β and γ subunits

*Correspondence to: Ben AVINER
E-mail: aviner@bgu.ac.il

doi: 10.1111/jcmm.12877

have a modulatory effect on the ionic flux *via* α_1 (for review, [33, 34]), including its kinetic properties and voltage dependence. For example, the β_{2a} subunit slows channel inactivation in many subunit combinations. On the other hand, the coexpression of $\alpha_2\delta$ subunits [35, 36] and γ subunits [37] has a smaller functional effect. Lately, it has been suggested that the γ_2 subunit is regulating the $Ca_V2.2$ indirectly by counteracting $G\beta\gamma$-mediated effects such as slowing of activation and voltage-dependent inactivation [38]. Notwithstanding, a functional recombinant channel does not always require expression of all subunits.

Early findings of HP effects on VDCC currents were indirectly obtained (for review, see [39]) from various preparations [27, 40–44]. The sensitivity of the $Ca_V2.2$ channel to HP [40, 41] was suggested, while the $Ca_V2.1$ channel was rendered HP resistant [13, 17]. Furthermore, Talpalar *et al.* [28] have postulated, based on mathematical modelling of experimental synaptic depression at HP, that rat dentate gyrus synapse is composed of pressure-sensitive (probably $Ca_V2.2$-dependent) and pressure-resistant (probably $Ca_V2.1$-dependent) independent modules of releasable vesicles pools.

In another attempt to study the HP selectivity of real currents, we have lately recorded extracellularly two components of Ca^{2+} currents in frog presynaptic terminals [15]. Partial pharmacologic identification has suggested that a fast component is N-type like and a slow component is probably one of the L-type channels. Hyperbaric pressure differentially affected the currents; the fast Ca^{2+} currents being highly depressed, while the slow Ca^{2+} currents were much less inhibited.

The difficulty in positively identifying the Ca^{2+} currents in *ex vivo* experimental tissues, the presence of more than one type of current in each neuron either in the presynaptic terminals or soma and dendrites, the diversity of channels in various preparations and the technical difficulties in performing the pressure experiments have presented us with a major challenge. We have, therefore, embarked on a long-term study that was aimed at overcoming these obstacles: direct measurement of VDCC currents by expressing the genetically identified cRNAs of the channels in frog oocytes under HP conditions. Recently, we have performed such a study for the first time on VDCCs currents of $Ca_V1.2$ and $Ca_V3.2$ [30], demonstrating selective and sometimes transient HP effects on the channels: $Ca_V1.2$ being potentiated, while the $Ca_V3.2$ is depressed.

In the present report, we extended our study to include two additional VDCCs, $Ca_V2.1$ and $Ca_V2.2$, which are mainly, but not exclusively, present at the neuronal presynaptic terminals. It is hoped that comprehensive understanding of the behaviour of each VDCC at HP will enable us to refine a model of activity [39] based on known channels spatial distribution along the neurons. This could elucidate the HPNS mechanism and may enable us to reduce or even eliminate its short- and long-term consequences.

Materials and methods

Oocytes extraction and cRNA injection

Oocytes of a *Xenopus laevis* mature female frog were surgically extracted from its ovary and treated with 1.5 mg/ml collagenase for 30–60 min. to remove connecting tissue. Suitable oocytes were sorted out by size, quality and developmental stage (VI), and kept in NDE96 solution containing (in mM): 96 NaCl, 2 KCl, 1 $MgCl_2$, 1 $CaCl_2$, 2.5 sodium pyruvate; 50 μg/ml gentamycin; 5 HEPES pH 7.5. Handling of frogs and oocytes extraction procedure were approved by the Ben-Gurion University of the Negev's ethics committee for the care and the use of animals and are in compliance with international laws and policies.

cRNAs of the subunits of PQ or N-type Ca^{2+} channels ($Ca_V2.1$ or $Ca_V2.2$, respectively) were synthesized from human, rat, mouse and rabbit cDNA by *in vitro* transcription with T7 or SP6 Amplicap High-Yield Message Maker Kit (Epicentre Technologies, Madison, WI, USA). Oocytes were then injected with the specific cRNA mix (2.5 ng) encoding for the pertinent subunits to express $Ca_V2.1$ or $Ca_V2.2$ and were kept in an incubator for 4–5 days at 18°C in NDE96 solution. The following subunits were used: $\alpha_{1A}+\beta_3+\alpha_2\delta$, comprising the $Ca_V2.1$; and $\alpha_{1B}+\beta_3+\alpha_2\delta$ or $\alpha_{1B}+\beta_3+\alpha_2\delta+\gamma_2$, comprising the $Ca_V2.2$.

Electrophysiological recordings

Four to five days after injection, the oocytes were placed in a specially designed bath, and two-electrode voltage clamp experiments with 10-mV increments and 5-sec. interval between −70 and 40 mV were performed inside a compression chamber, utilizing an AXOCLAMP 2B amplifier (Molecular Devices, Axon Instruments, Inc., CA, USA), WinWCP pulse generating software by Strathclyde University, Axon Instruments DIGIDATA 1322A, and AxoScope 9.2 software. Sharp glass electrodes were fabricated using Sutter Instrument P-1000 micropipette puller, filled with 3 M KCl, tip resistance <1.5 MΩ. The oocytes were penetrated by the electrodes, and only then the bath was carefully inserted into the chamber, slid onto an electric socket with preinstalled wires crossing the chamber wall. While in the chamber, each oocyte was continuously perfused with a Ba^{2+} solution containing (in mM): 20–40 $Ba(OH)_2$, 50 NaOH, 2 KOH and 5 HEPES, titrated to pH 7.5 with methanesulfonic acid. Ba^{2+} was used as charge carrier, replacing the Ca^{2+} ions, to avoid Ca^{2+}-dependent inactivation and the activation of Ca^{2+}-activated Cl^- channels (Cl^-_{Ca}), known to be endogenously expressed in oocyte membrane [45]. We have recently demonstrated in identical experimental system that blocking the Cl^-_{Ca} current does not interfere with the HP effect on VDCCs [30]. Both $Ca_V2.1$ and $Ca_V2.2$ also have higher conductance to Ba^{2+} [46], allowing measurement of minute currents that otherwise would have been unnoticed. The solution, saturated with air at atmospheric pressure, was introduced into the chamber by the use of a high-pressure pump (Minipump; LDC Analytical Inc., Riviera Beach, FL, USA) at room temperature (24–25°C), at a rate of 1.5–2 ml/min. Temperature was constantly monitored throughout the experiments by the use of a thermistor submerged in the solution in the vicinity of the oocyte groove. Deviation of only ±0.5°C was allowed from the control temperature for later measurements. We have also demonstrated in our recent study [30] that the small reversible adiabatic temperature changes are not responsible for the response of the VDCCs to HP. In addition, we have proved that the voltage and currents measurements in our setup are stable along the relatively long duration of compression and decompression. Typical recorded traces are shown in Figure 1. Voltage traces are not 'command voltages' but rather the actual recording of the oocyte transmembrane potential. Holding potential was −80 mV (see example in Fig. 1A). The duration of each depolarizing step was 500 msec., which

Journal of Cellular and Molecular Medicine published by John Wiley & Sons Ltd and Foundation for Cellular and Molecular Medicine.

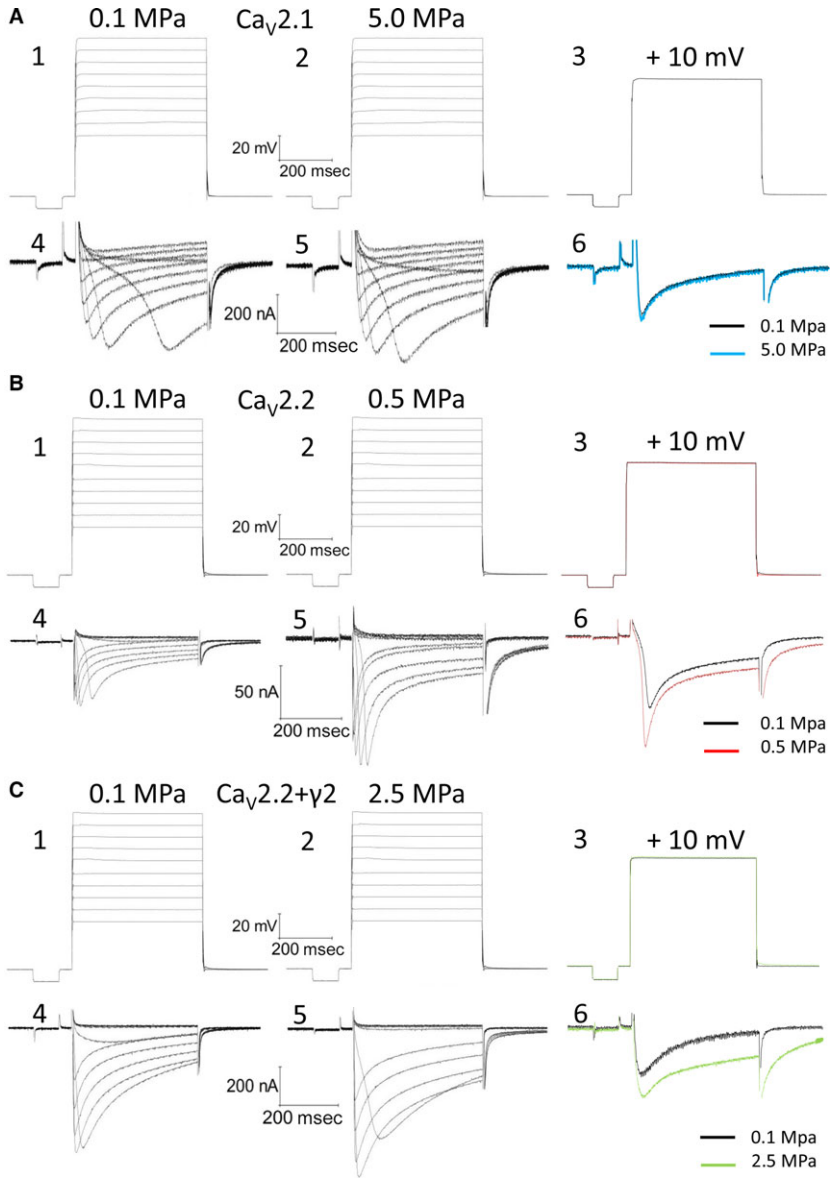

Fig. 1 Ba^{2+} currents recorded in $Ca_V2.1$ (**A**), $Ca_V2.2$ (**B**) and $Ca_V2.2_{+\gamma2}$ (**C**) channels. A1-3, B1-3, C1-3, depolarization steps for A4-6, B4-6 and C4-6, respectively. A4-5, B4-5, C4-5, currents at 0.1 and at HP, the exact pressure is indicated. A6, B6, C6, superimposed single current traces recorded under normobaric and hyperbaric conditions, generated by identical superimposed depolarization to 10 mV.

was preconditioned by a 100-msec. hyperpolarizing step to −90 mV to release the VDCC from partial inactivation. The latter was also used to calculate and monitor the oocytes' instantaneous input resistance for measuring and subtracting the leak currents, which were accounted for at each recorded trace separately, thus unmasking the net VDCC current.

Every series of depolarizing pulses was used to construct an I-V curve and repeated at least three times to verify stability of the currents, as was previously described (fig. 1 in [30]). Recorded traces with voltage fluctuation greater than 2 mV during depolarization were disregarded. We studied HP effects on I-V curve, maximal currents, activation and inactivation functions, channel kinetics such as time to peak (TTP) and time constants (τ), and voltage dependency. Maximal currents were measured at the minimal point of the current curve. Inactivation (I/Imax) was measured towards the end of the depolarizing step in comparison to the measured maximal current (as above). A fit was calculated for each decaying section of the current in every recorded trace according to a biexponential equation [47] defining two time constants for decay:

$$\text{Fit} = -\text{A1}\exp(-t/\tau_{\text{Decay Fast}}) - \text{A2}\exp(-t/\tau_{\text{Decay Slow}}) + \text{C}$$

For the rising phase and the tail currents, a single exponential fit was performed. All fits were calculated between the curves' normalized values of 0.1 and 0.9.

Activation volume ($\Delta V^{\ddagger}$) was calculated for time constants of channel activation, inactivation and deactivation under normobaric and hyperbaric conditions, following the known equation [48]:

$$\Delta V^{\ddagger} = RT(\partial \ln \tau/\partial P)_T$$

Helium compression

After control measurement taken at 0.1 MPa, compression steps to 0.5, 2.5 and 5.0 MPa were performed by compressed helium. Compression was done manually at a rate of approximately 0.25–0.5 MPa/min. and never exceeded 1.0 MPa/min. Helium was used instead of air due to its inert quality and the need to avoid known nitrogen narcosis and oxygen toxicity–related effects [49]. Principally, compression with helium does not change the other gases (primarily oxygen and nitrogen) partial pressure. Here, the chamber gaseous content was flushed with helium during compression due to the need to drain the excess of physiological solution, and thus the oxygen and nitrogen partial pressure was reduced over time. However, the oocytes were continuously perfused with fresh solution equilibrated with air at 0.1 MPa, and thus the oocytes were exposed to normal partial pressure of oxygen and nitrogen. All pressure units are absolute.

Statistical analysis

The full set of parameters was calculated off-line for each recorded trace separately, considering the instantaneous input resistance and leak currents where appropriate, using a dedicated self-designed Matlab software program. The data were exported to Microsoft Excel software (Microsoft Corp., Redmond, WA, USA). Repetitive measurements of I-V curves, verifying stability of the measured currents, were averaged and used as a single value for each depolarization step, which in turn was used for averaging with results from other oocytes. The same was done for all other parameters. Each oocyte was used as its own control, and thus values were normalized to 0.1 MPa when needed. When data from more than one oocyte were pooled, binning was performed relative to the voltage generating the maximal current in the I-V curve (V_{Imax}); hence, in figures representing these data (Figs 2–9B, D and F), the *X*-axis title is ΔV. The actual X values in all figures were determined by averaging the actual recorded voltages during depolarizing steps. Hence, minor shifts of 1–2 mV from the values indicated in the *X*-axis may occur. Paired sample *t*-test was used to analyse the significance of the results: each pooled value was compared with its pertinent pooled value at 0.1 MPa for the same ΔV. Significant difference ($P < 0.05$) is represented by asterisks in figures.

Results

Unaffected current in $Ca_V2.1$

As expected, the amplitude of Ba^{2+} currents in $Ca_V2.1$ was not affected in oocytes exposed to HP (2.5–5.0 MPa, see example in Fig. 2A). Comparing the normalized maximal currents (negative peak in I-V curve) at V_{Imax} shows that compression to 2.5 and 5.0 MPa did not significantly change the maximal currents ($-8 \pm 10\%$ and $-2 \pm 3\%$, respectively, $P > 0.4$, $n = 7$–9, Fig. 2B). Decompression to 0.1 MPa also did not significantly affect the maximal current; it remained slightly depressed by $-14 \pm 6\%$ ($P > 0.3$, $n = 6$). Neither the threshold voltage nor V_{Imax} were affected by HP.

Augmented current in $Ca_V2.2$

Surprisingly, Ba^+ currents in $Ca_V2.2$ were significantly increased at HP (0.5–5.0 MPa) in a dose-dependent manner (see example in Fig. 2C), in contrast to the expectations based on previous studies (see Introduction). Compression to 2.5 and 5.0 MPa caused a similar augmentation of the maximal currents at V_{Imax} by $132 \pm 54\%$ and $123 \pm 8\%$ of control values, respectively (Fig. 2D, average $\pm$ SEM, $P < 0.01$, $n = 7$–9); therefore, lower HP steps to 1.1 MPa and 0.5 MPa were performed in subsequent experiments in order to reveal the threshold for HP effect. However, the maximal current at 1.1 MPa was augmented in a similar manner by $122 \pm 56\%$ ($P < 0.01$, $n = 3$, data not shown), and only a lower HP perturbations to 0.5 MPa had a weaker effect on the maximal currents at V_{Imax}: a $61 \pm 16\%$ augmentation ($P < 0.05$, $n = 12$). Neither the threshold voltage nor the V_{Imax} were affected by HP. Decompression to 0.1 MPa only partially recovered the current, which remained augmented by $73 \pm 15\%$ ($P < 0.05$, $n = 7$).

$Ca_V2.2$ expressed including the γ_2 subunit

The functionality of a recombinant channel is vastly dependent on the subunits constructing it, their type and isoforms, *etc.* The unexpected HP-induced current augmentation in the $Ca_V2.2$ led us to speculate whether this recombinant channel is affected differently by HP than the native one. In order to elucidate this issue, we have repeated the experiments following expression of the $Ca_V2.2$ including the one subunit that was excluded thus far as it is not essential for the channels' functionality, the γ_2. Although identifying it as a classic subunit of this channel is still debatable, its role in modulating it is not [38, 50].

Indeed, the $Ca_V2.2$ expressed including the γ_2 subunit ($Ca_V2.2_{+\gamma2}$) has reacted differentially to HP perturbation. For example, the augmentation of currents witnessed in the $Ca_V2.2$ was substantially subsided (Fig. 2E and F).

Channels' conductance

The cumulative conductance for the population of the channels ('input conductance' of the oocyte) calculated relatively to the membrane potential shows similar results to the general findings in the I-V curves (see examples in Fig. 3A, C and E). High HP (2.5–5.0 MPa) increased the conductance in the $Ca_V2.2$ and $Ca_V2.2_{+\gamma2}$ channels (Fig. 3D and F) but did not have a consistent effect in the $Ca_V2.1$ channel (Fig. 3B). On average, the change from threshold to maximal normalized response occurred within a 50-mV depolarization range for the $Ca_V2.2$ and $Ca_V2.2_{+\gamma2}$ channels and only 30 mV for the $Ca_V2.1$ channel.

Currents inactivation

We have previously demonstrated that in the absence of Ca^{2+} ions in the solution, the Ca^{2+}-dependent inactivation of these VDCC is

Journal of Cellular and Molecular Medicine published by John Wiley & Sons Ltd and Foundation for Cellular and Molecular Medicine.

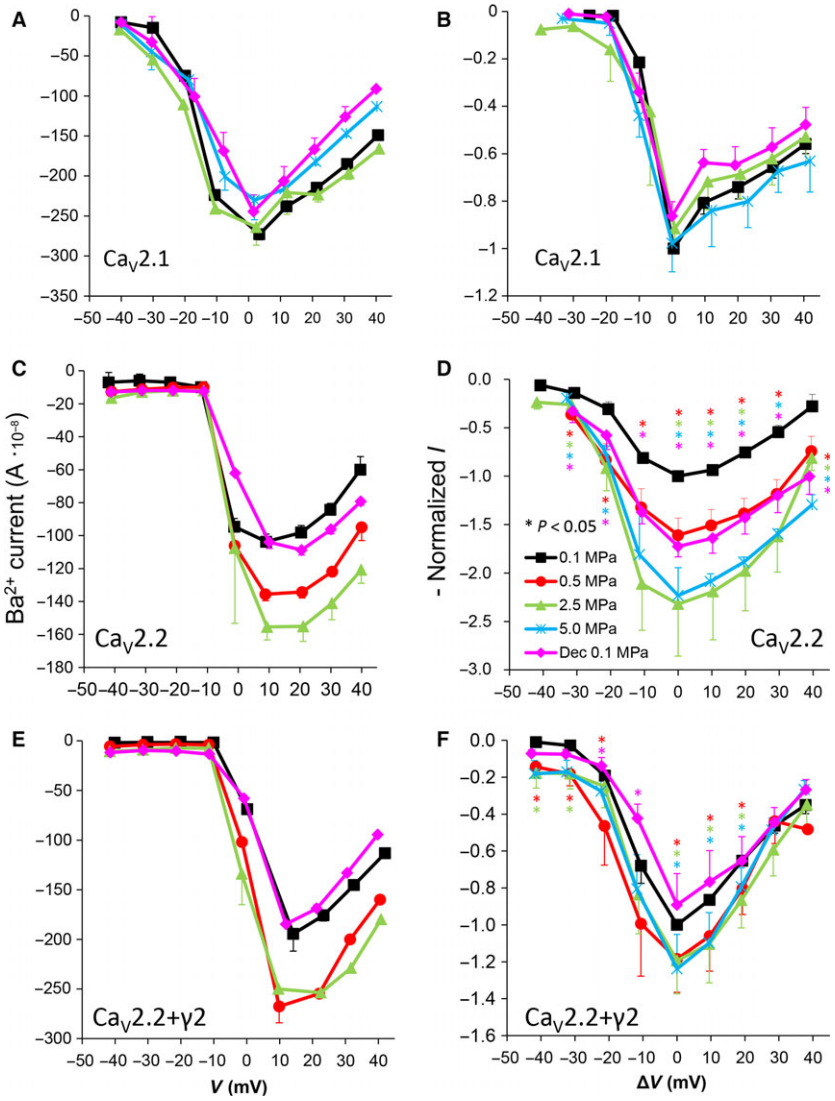

Fig. 2 I-V curves of maximal currents. (**A** and **B**) $Ca_V2.1$, (**C** and **D**) $Ca_V2.2$, (**E** and **F**) $Ca_V2.2_{+\gamma2}$ channels. (**A**, **C** and **E**) I-V curve of a single oocyte. (**B**, **D** and **F**) Pooled data from 7–9 (**B**), 9–12 (**D**) and 7–10 (**F**) oocytes exposed to 0.5–5.0 MPa pressure (colour indicated), normalized to maximal current at 0.1 MPa, holding potential is adjusted [ΔV (mV)] so that 0 indicates the potential at which maximal current is obtained (V_{Imax}). Statistical significance for each point on the curve is indicated by corresponding colour asterisks ($P < 0.05$). Dec indicates decompression.

eliminated [30], leaving only the voltage- and time-dependent inactivation that can be evaluated as the ratio between the remaining current at the end of the depolarizing voltage step and its maximal value (I_{end}/I_{max}; see examples in Fig. 4A, C and E). All channels demonstrated a greater inactivation at strong depolarizations, as expected for these VDCCs. For the $Ca_V2.1$ channel, HP did not have a consistent or significant effect on inactivation (Fig. 4B). For the $Ca_V2.2$ channel, inactivation tended to be stronger when large currents were evoked (ΔV −10 to 20 mV) at HP, but was weakened by it around threshold voltage or towards the reversal potential (*e.g.* ΔV −20, 40 mV, respectively). Decompression relieved that effect (Fig. 4D). For the $Ca_V2.2_{+\gamma2}$ channel, inactivation was weakened at HP of 2.5–5.0 MPa at the whole voltage range of the channel activity, but only at a narrower voltage range (ΔV −10 to V_{Imax}) at 0.5 MPa (Fig. 4F). Decompression did not recover inactivation to control values.

Currents kinetics: time to peak

We have recently demonstrated that HP can affect the kinetics of VDCC current (Aviner *et al.*) [30]. If the VDCC kinetic parameters such as the rates of activation, inactivation and deactivation of the current are affected by HP, that may change the maximal current and the total ionic flux through the channel. We have, therefore, measured the time passing from the stimulating depolarizing step to the development of I_{max} (TTP). Examples can be seen in Figure 5A, C and E. Time to peak was not altered by HP in the $Ca_V2.1$ channel, excluding a tendency for an increase at V_{Imax} at 5.0 MPa, nor was it changed by decompression (Fig. 5B). It can be seen that a barely threshold depolarization led to a longer TTP value due to the indecisive recruitment of the channels population. For the $Ca_V2.2$ channel, the HP effect on TTP was complex. At 0.5 MPa,

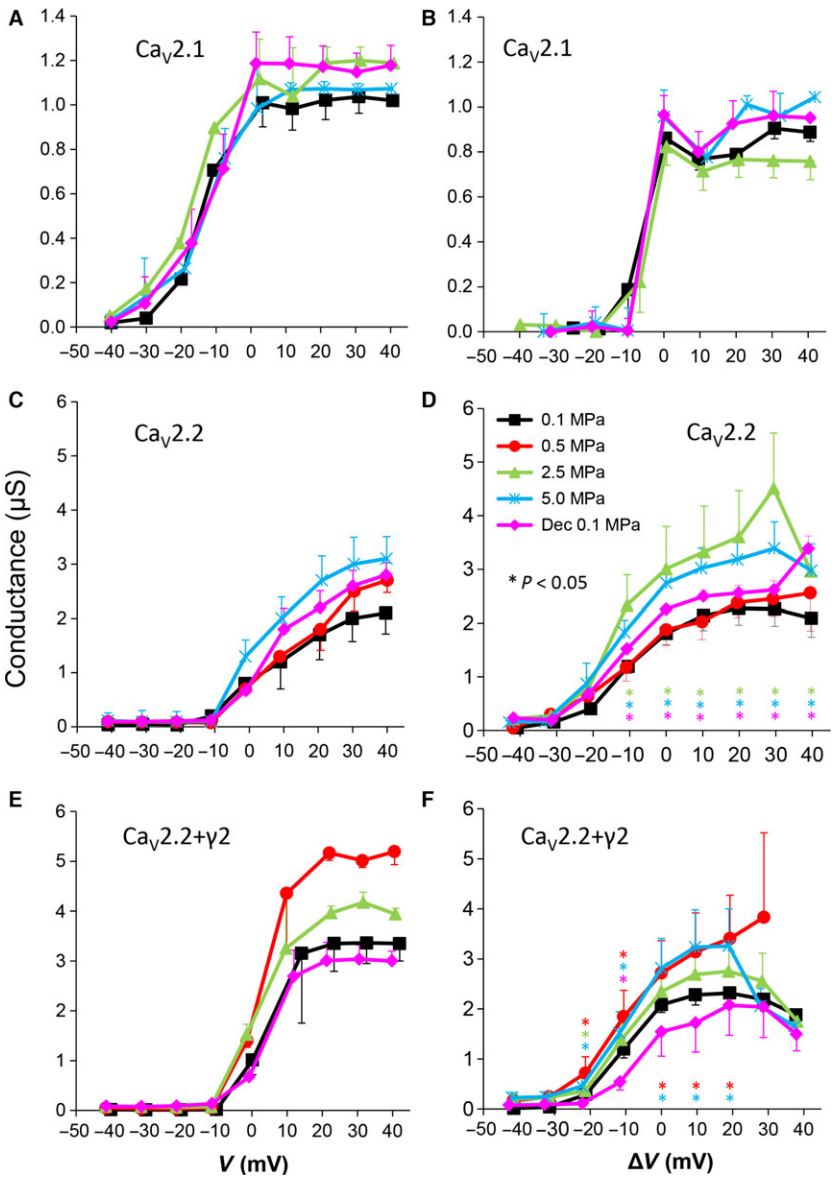

Fig. 3 Channels' conductance at various pressures. (**A** and **B**) $Ca_V2.1$, (**C** and **D**) $Ca_V2.2$ and (**E** and **F**) $Ca_V2.2_{+\gamma2}$ channels. (**A**, **C** and **E**) Conductance measured in a single oocyte. (**B**, **D** and **F**) Pooled data of the channels, *n* as stated in Figure 2. Statistical significance for each point on the curve is indicated by corresponding colour asterisks. Holding potential [ΔV (mV)] is expressed as in Figure 2. Dec indicates decompression.

TTP was decreased; at 2.5 MPa, it was decreased for V_{Imax} and up to ΔV 20 mV, but increased below V_{Imax}; and at 5.0 MPa, it was slightly increased below V_{Imax} range (Fig. 5D). Decompression recovered TTP to control values. For the $Ca_V2.2_{+\gamma2}$ channel, TTP was elongated up to ΔV 20 mV, more clearly at high HP (2.5, 5.0 MPa).

Currents kinetics: τ_{Rise}

The time constant of the rising phase of the current, τ_{Rise}, is another useful parameter to evaluate the activation of the current (Fig. 6A, C and E). Hyperbaric pressure of 5.0 MPa elongated τ_{Rise} of $Ca_V2.1$ at a narrow depolarization range (ΔV −10 to V_{Imax}), whereas at 2.5 MPa, it showed no significant change (Fig. 6B). The maximal increase in τ_{Rise} of $Ca_V2.2$ was at 2.5 MPa at a wider depolarization range (ΔV −10 to 10 mV), whereas a smaller change was observed at 5.0 MPa (Fig. 6D). Hyperbaric pressure had almost no statistically significant effect on τ_{Rise} in the $Ca_V2.2_{+\gamma2}$ channel. Decompression recovered τ_{Rise} back to control levels in all channels.

Currents kinetics: fast τ_{Decay}

A change in the inactivation value (I_{end}/I_{max}) could originate from an effect on the channels' rate of decay, as I_{end} is measured at the end of

Journal of Cellular and Molecular Medicine published by John Wiley & Sons Ltd and Foundation for Cellular and Molecular Medicine.

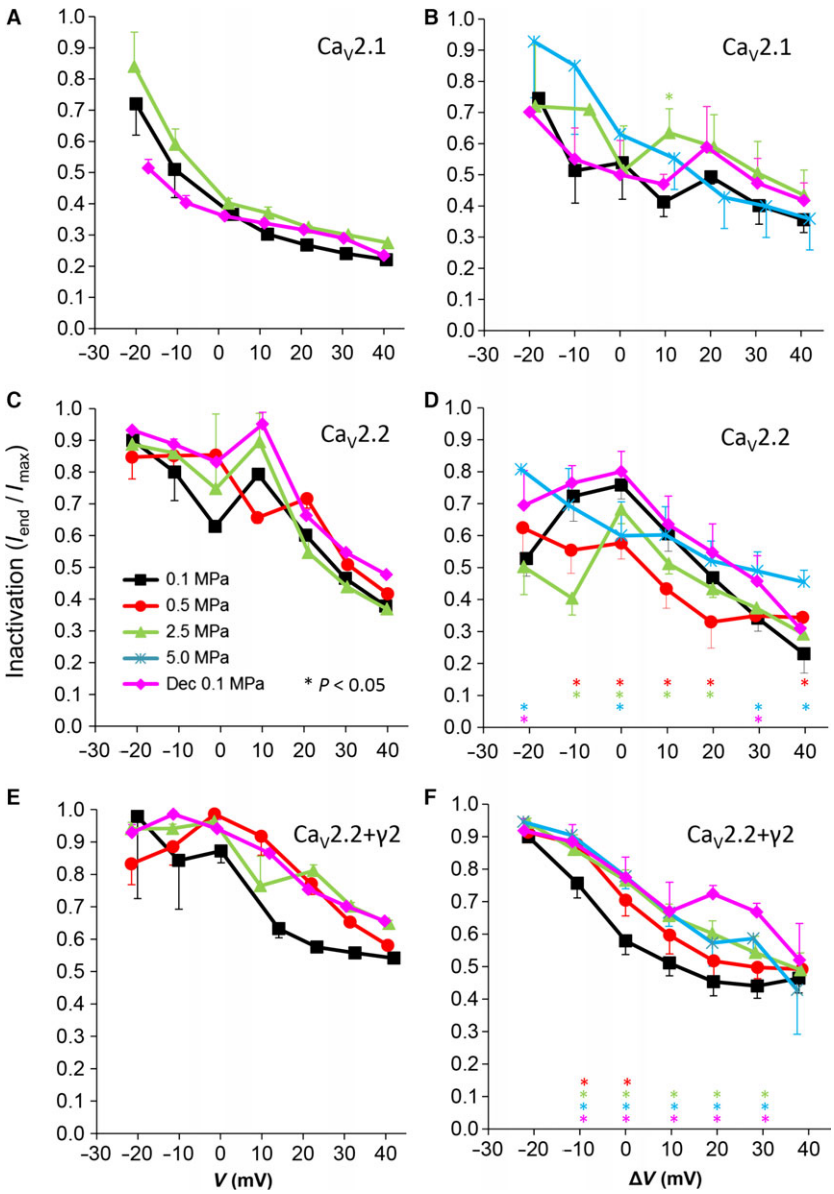

Fig. 4 Voltage- and time-dependent current inactivation (I_{end}/I_{max}) at various pressures. (**A** and **B**) $Ca_V2.1$, (**C** and **D**) $Ca_V2.2$ and (**E** and **F**) $Ca_V2.2_{+\gamma2}$ channels. (**A**, **C** and **E**) Inactivation measured in a single oocyte. (**B**, **D** and **F**) Pooled data of the channels, *n* as stated in Figure 2. Pressures are colour indicated. Statistical significance for each point on the curve is indicated by corresponding colour asterisks. Holding potential [ΔV (mV)] is expressed as in Figure 2. Dec indicates decompression.

the depolarizing step and not under steady-state conditions. The decay of VDCCs current is known to have two time constants, fast and slow, which are commonly attributed to voltage and Ca^{2+} inactivation, respectively. However, even with Ba^{2+} as the charge carrier, the decaying current could not be fitted satisfactorily using a single exponent.

For the $Ca_V2.1$, as expected by the lack of consistent change in inactivation, HP did not cause a clear change in the fast τ_{Decay} ($\tau_{Decay\ fast}$; Fig. 7A and B). For the $Ca_V2.2$, a considerable shortening of $\tau_{Decay\ fast}$ at HP was observed throughout the activity range of the channel even at 0.5 MPa (Fig. 7C and D), while decompression generally relieved this effect. The HP effect was reversed in the $Ca_V2.2_{+\gamma2}$ channel, where $\tau_{Decay\ fast}$ was elongated (Fig. 7F).

Currents kinetics: slow τ_{Decay}

The slow τ_{Decay} ($\tau_{Decay\ Slow}$) in all channels was elongated by stronger depolarizations at 0.1 MPa (Fig. 8A, C and E), similarly to previous findings in VDCCs [30]. For the $Ca_V2.1$ channel, the $\tau_{Decay\ Slow}$ was almost entirely not affected by HP, as may be predicted by inconsistent effect on its inactivation (Fig. 8A and B). For the $Ca_V2.2$ channel, $\tau_{Decay\ Slow}$ was shortened by high HP (2.5–5.0 MPa) at suprathreshold depolarization (ΔV −10 mV and above), but compression to lower HP of 0.5 MPa led to a mixed effect: generally elongating $\tau_{Decay\ Slow}$ below V_{Imax} and shortening it above V_{Imax}. Decompression eliminated this effect almost entirely (Fig. 8C and D). In the $Ca_V2.2_{+\gamma2}$ channel, the effect of high HP (2.5–5.0 MPa) was also reversed,

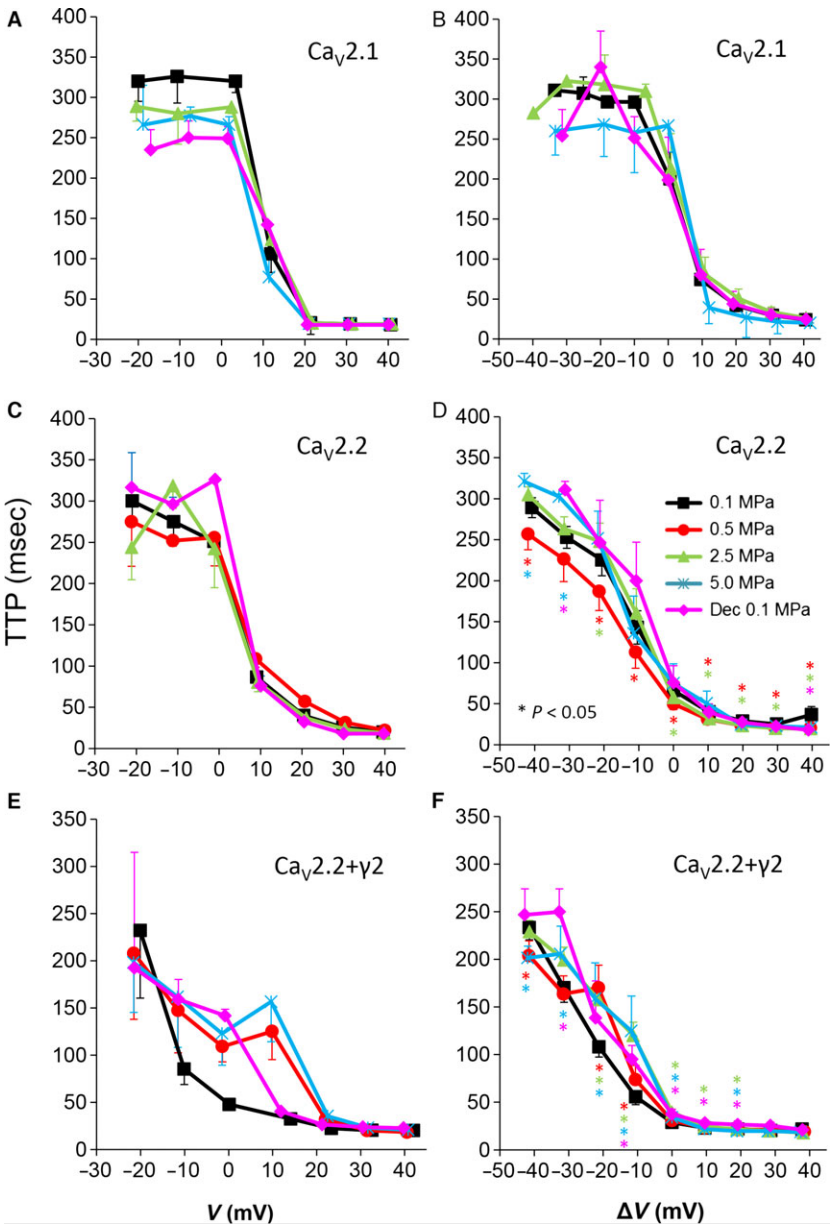

Fig. 5 Time to current peak (TTP) from stimulus onset at various pressures. (**A** and **B**) $Ca_V2.1$, (**C** and **D**) $Ca_V2.2$ and (**E** and **F**) $Ca_V2.2_{+\gamma2}$ channels. (**A**, **C** and **E**) TTP measured in a single oocyte. (**B**, **D** and **F**) Pooled data of the channels, *n* as stated in Figure 2. Pressures are colour indicated. Statistical significance for each point on the curve is indicated by corresponding colour asterisks. Holding potential [ΔV (mV)] is expressed as in Figure 2. Dec indicates decompression.

elongating $\tau_{Decay\ Slow}$ above V_{Imax}, but low HP (0.5 MPa) had no effect (Fig. 8E and F). Decompression only partially relieved the HP effect.

Currents kinetics: τ_{Tail}

The tail current time constant (τ_{Tail}), representing the kinetics of the channels' deactivation, was shortened by increasing depolarization in all channels (see example in Fig. 9A, C and E). Hyperbaric pressure elongated τ_{Tail} in the $Ca_V2.2$ and $Ca_V2.2_{+\gamma2}$ channels almost throughout their activity range (Fig. 9D and F), but only up to V_{Imax} in the $Ca_V2.1$ (Fig. 9B). Decompression recovered τ_{Tail} in $Ca_V2.1$, but not so much in the $Ca_V2.2$s; τ_{Tail} remained elongated at depolarizations below ΔV 20 mV in the $Ca_V2.2$ channel and below V_{Imax} in the $Ca_V2.2_{+\gamma2}$ channel.

Activation volume ($\Delta V^{\ddagger}$)

$\Delta V^{\ddagger}$ values were calculated from the change in the rate of processes under hyperbaric conditions compared with control

Journal of Cellular and Molecular Medicine published by John Wiley & Sons Ltd and Foundation for Cellular and Molecular Medicine.

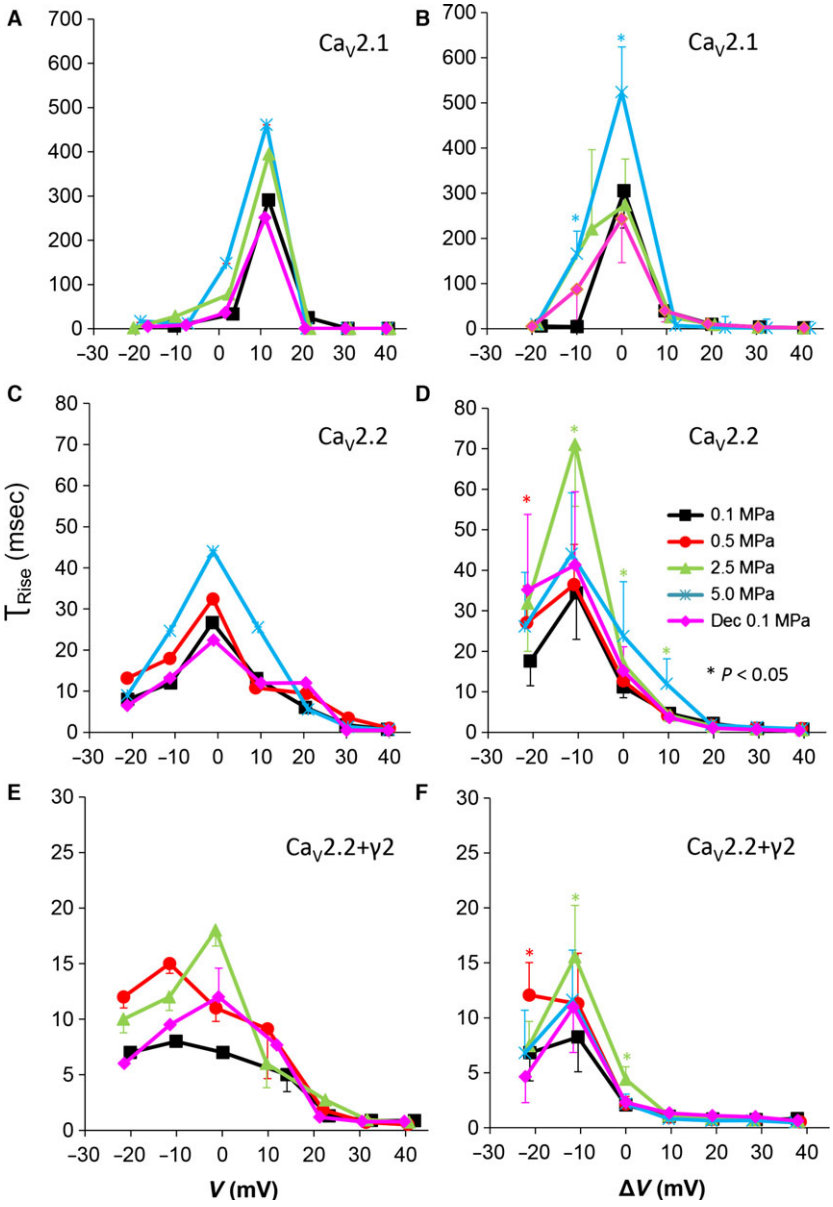

Fig. 6 Time constant of current activation (τ_{Rise}) at various pressures. (**A** and **B**) $Ca_V2.1$, (**C** and **D**) $Ca_V2.2$ and (**E** and **F**) $Ca_V2.2_{+\gamma2}$ channels. (**A**, **C** and **E**) τ_{Rise} measured in a single oocyte. (**B**, **D** and **F**) Pooled data of τ_{Rise}, *n* as stated in Figure 2. Pressures are colour indicated. Statistical significance for each point on the curve is indicated by corresponding colour asterisks. Holding potential is expressed [ΔV (mV)] as in Figure 2. Dec indicates decompression.

pressure, as described in the Materials and methods. $\Delta V^{\ddagger}$ serves as a tool for assessing the sensitivity of a molecule to pressure perturbation, quantifying it in comparable values. Table 1 summarizes $\Delta V^{\ddagger}$ values for the tested VDCCs for 2.5 MPa. Generally, the results correspond to both sensitivity and trend of the changes described above.

A summary of HP effects on these channels is given in Table 2. Overall, $Ca_V2.1$ was not significantly affected by HP, whereas the $Ca_V2.2$s channels were HP sensitive. Although I_{max} and the conductance showed the same trend, interestingly excluding τ_{Tail}, all other parameters measured in $Ca_V2.2_{+\gamma2}$ demonstrated an altered response to HP compared with $Ca_V2.2$: decreased inactivation value, increased $\tau_{Decay\ Fast}$ and $\tau_{Decay\ Slow}$, and unaffected τ_{Rise} (Table 2).

Discussion

Current activation

Currents' amplitude

As demonstrated in our previous direct [30] and indirect [15, 20] measurements of currents in VDCCs at HP, pressure effect can be selective. In this study, we report that currents through $Ca_V2.2$ are

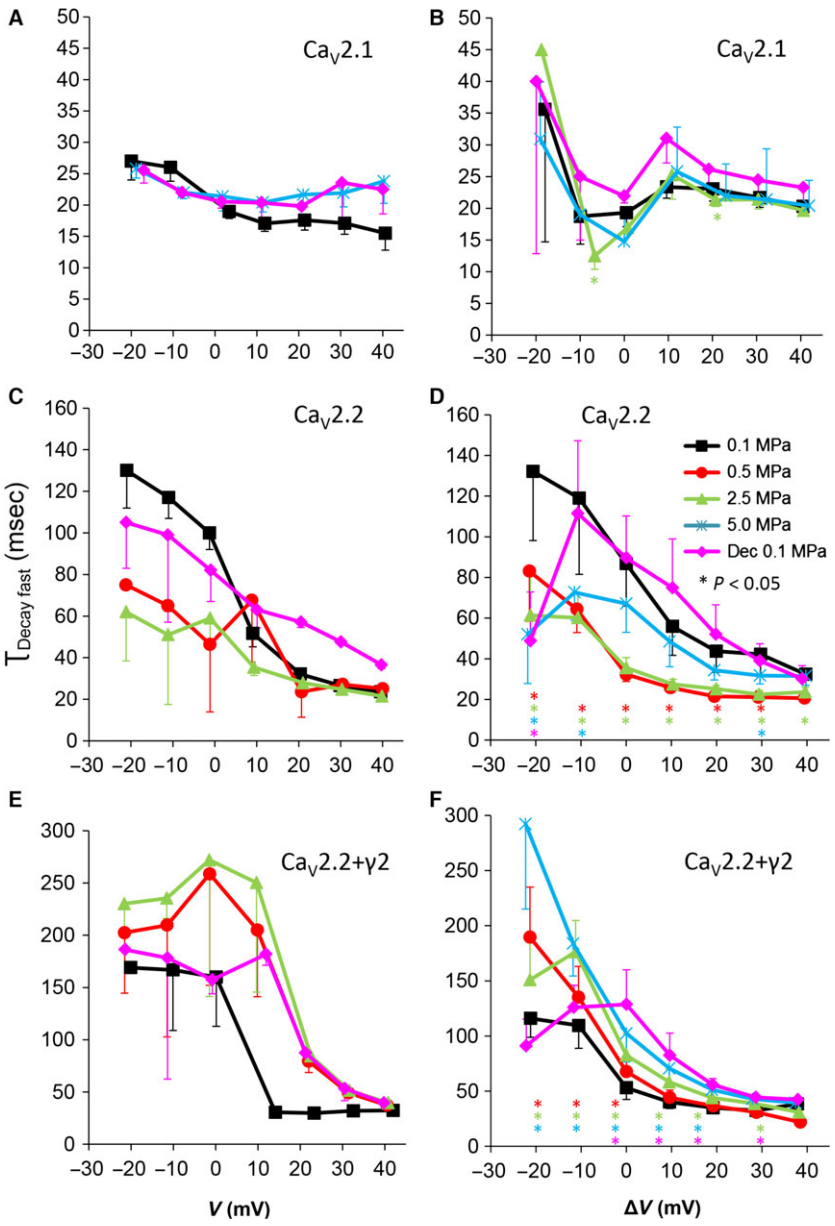

Fig. 7 Fast time constant of voltage- and time-dependent current inactivation ($\tau_{Decay\ Fast}$). (**A** and **B**) $Ca_V2.1$, (**C** and **D**) $Ca_V2.2$, (**E** and **F**) $Ca_V2.2_{+\gamma2}$ channels. (**A**, **C** and **E**) $\tau_{Decay\ Fast}$ measured in a single oocyte. (**B**, **D** and **F**) Pooled data of the channels, *n* as stated in Figure 2. Pressures are colour indicated. Statistical significance for each point on the curve is indicated by corresponding colour asterisks. Holding potential [ΔV (mV)] is expressed as in Figure 2. Dec indicates decompression.

increased, whereas currents through the $Ca_V2.1$ channel are generally unaffected by HP. Only a partial recovery in the amplitude of the currents in the $Ca_V2.2$ was witnessed on return to atmospheric pressure.

The effect of HP found here on the $Ca_V2.1$ channel conforms with previous findings [17], whereas the HP effect on the $Ca_V2.2$ is in contrast to previous reports that suggested reduction in Ca^{2+} influx through $Ca_V2.2$ [40, 41]. Considering the fact that the channels tested here are recombinant and comprised human and rabbit genetic material (*versus* native intact lobster and guinea pig preparations), the diversity of VDCCs types and their isoform, the unique HPNS threshold for each animal species and the knowledge that even one amino acid alteration can significantly change the whole protein functionality, this contrast is not necessarily surprising. It, in fact, stresses that the interaction between the channels' subunits may have an impact on the way the channel will react to HP perturbation. In our experiments, we used Ba^{2+} and tested only the voltage- and time-dependent inactivation, whereas the previous findings mentioned above were *in situ*, where Ca^{2+} was the ion carrying the current. If a Ca^{2+}-dependent inactivation of the current, known to be stronger than the voltage- and time-dependent one, is increased at HP, the overall effect could be depression of the maximal current, explaining the difference in the HP effect between the present and previous studies.

Journal of Cellular and Molecular Medicine published by John Wiley & Sons Ltd and Foundation for Cellular and Molecular Medicine.

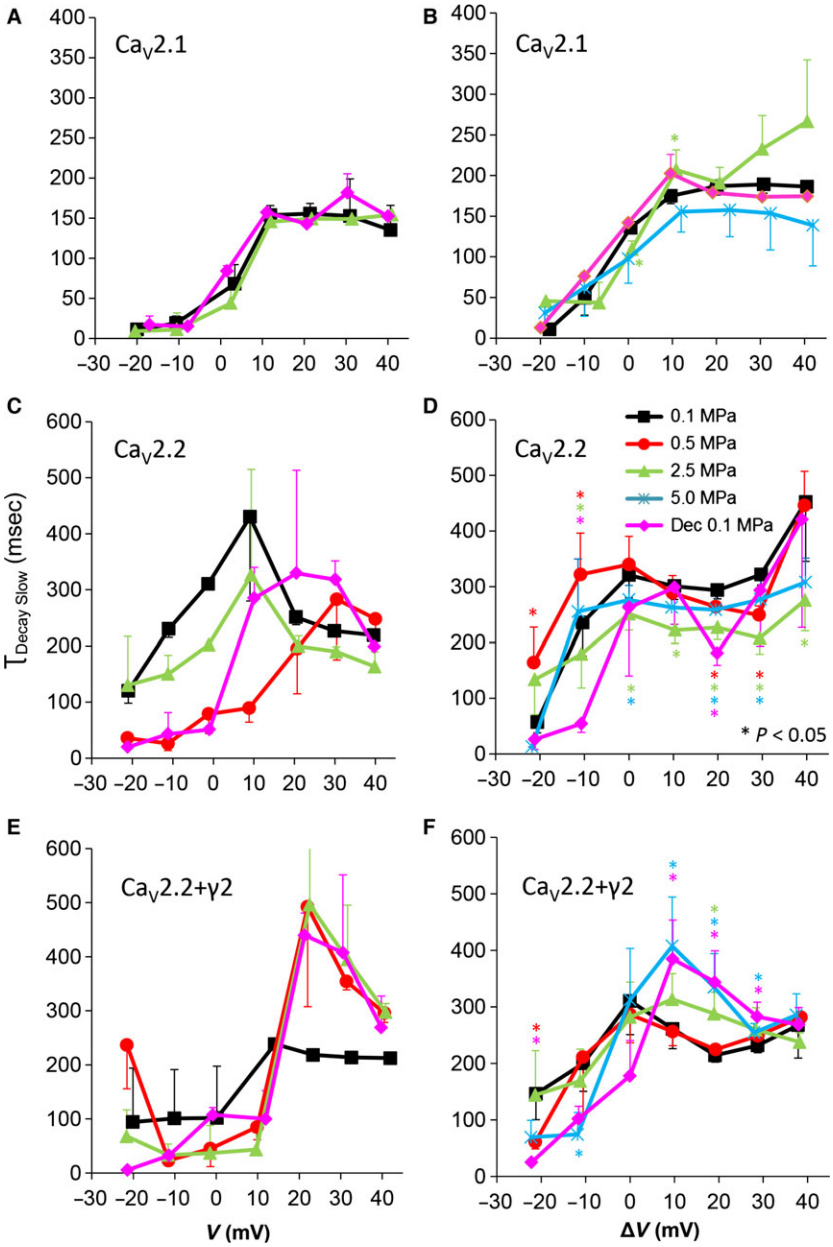

Fig. 8 Slow time constant of voltage- and time-dependent current inactivation ($\tau_{Decay\ Slow}$). (**A** and **B**) $Ca_V2.1$, (**C** and **D**) $Ca_V2.2$ and (**E** and **F**) $Ca_V2.2_{+\gamma2}$ channels. (**A**, **C** and **E**) $\tau_{Decay\ Slow}$ measured in a single oocyte. (**B**, **D** and **F**) Pooled data of the channels, *n* as stated in Figure 2. Pressures are colour indicated. Statistical significance for each point on the curve is indicated by corresponding colour asterisks. Holding potential [ΔV (mV)] is expressed as in Figure 2. Dec indicates decompression.

On the other hand, the increase in the currents' maximal amplitude in $Ca_V2.2$ channel at HP in this work is similar to HP effect found recently in $Ca_V1.2$ [30] and reminiscent of the 'delayed rectifier' K^+ channels (another member of this protein superfamily) in which the non-inactivating currents were greater at steady state during HP exposure in invertebrates such as squid [51–53], snail [54] and lobster [55].

Both $Ca_V2.1$ and $Ca_V2.2$ channels are mainly expressed at the presynaptic nerve terminals [56, 57] and are involved in neurotransmitters release [58]. However, $Ca_V2.2$ channel is also expressed in dendrites and cell bodies of neurons, *e.g.* in the rat dentate gyrus [59]. In such a case, increased channel activity may augment synaptic release and contribute to 'dendritic boosting' (increased transfer function between synaptic inputs and somatic spike generation) previously reported by our laboratory [60]. Such boosting, that conforms well to HPNS hyperexcitability, was attributed also to the $Ca_V1.2$ channel that is prevalent in the dendrites [30]. This process is an example of HP influence on neuronal networks that does not act through synaptic transmission. As mentioned above, increased $Ca_V2.2$ currents are quite unexpected. However, the current amplitude in the recombinant $Ca_V2.2_{+\gamma2}$ channel, considered to better resemble a native one, was much less affected; the average normalized

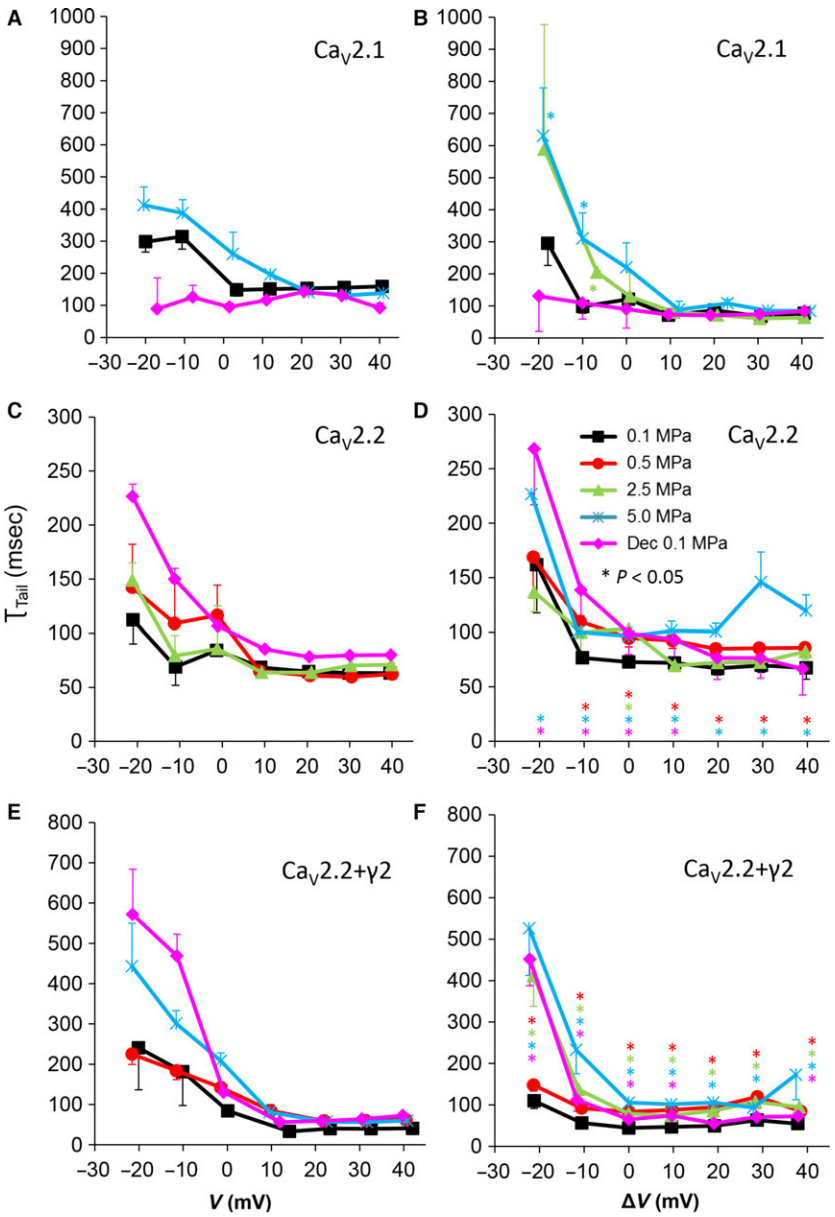

Fig. 9 Tail current time constant (τ_{Tail}) at various pressures. (**A** and **B**) $Ca_V2.1$, (**C** and **D**) $Ca_V2.2$ and (**E** and **F**) $Ca_V2.2_{+\gamma2}$ channels. (**A**, **C** and **E**) τ_{Tail} measured in a single oocyte. (**B**, **D** and **F**) Pooled data of τ_{Tail}, *n* as stated in Figure 2. Pressures are colour indicated. Statistical significance for each point on the curve is indicated by corresponding colour asterisks. Holding potential [ΔV (mV)] is expressed as in Figure 2. Dec indicates decompression.

maximal current in V_{Imax} was increased by ~20% at 2.5–5.0 MPa, compared with ~125% increase for the same pressures of the $Ca_V2.2$. Thus, we may assume that some native $Ca_V2.2$ channel would be depressed by HP, similarly to the $Ca_V3.2$ channel (Aviner *et al.*) [30]. At present, we can attribute the synaptic pressure-resistant module (see Introduction) to the $Ca_V2.1$ channel activity; however, we cannot safely attribute the pressure-sensitive module (reduction in synaptic release) to the activity of any recombinant $Ca_V2.2$ channel that we have tested so far. Yet, as both channels are mainly expressed at the presynaptic nerve terminals and are involved in neurotransmitters release [58] (see Introduction), it may be postulated that the individual relative sensitivity or durability to HPNS development in humans may rise from different spatial distribution and quantitative expression of these channels in somatosensory and motor nerves.

Table 1 Activation volume values (ml/mole) at 2.5 MPa

$\Delta V^{\ddagger}$ (ml/mole)	τ_{Rise}	$\tau_{Decay\ Fast}$	$\tau_{Decay\ Slow}$	τ_{Tail}
$Ca_V2.1$	−111	−134	−223	73
$Ca_V2.2$	427	−922	−253	358
$Ca_V2.2_{+\gamma2}$	779	455	99	595

Journal of Cellular and Molecular Medicine published by John Wiley & Sons Ltd and Foundation for Cellular and Molecular Medicine.

Table 2 General qualitative effect of HP on measured channel characteristics

	I_{max}	Conductance	Inactivation	TTP	τ_{Rise}	$\tau_{Decay\ Fast}$	$\tau_{Decay\ Slow}$	τ_{Tail}
$Ca_V2.1$	=	=	=	=	=	=	=	↑(=)
$Ca_V2.2$	↑	↑	↑(↓)	↓/↑/=	=/↑/(=)	↓	↓	↑
$Ca_V2.2_{+\gamma2}$	↑	↑	↓	↑	=	↑	↑	↑

↑, increase; ↓, decrease; =, no change; ( ), stronger depolarization; /, higher HP.

Channels' conductance

Generally, the calculated conductance (input conductance) behaviour relative to the membrane potential at HP reflects the changes shown in the I-V curves: unaffected in $Ca_V2.1$ and increased in $Ca_V2.2$s (Fig. 3B, D and F). However, in the $Ca_V2.2$, compression to 0.5 MPa did not increase conductance, despite the augmented current measured. Such a phenomenon could be explained either by altered reversal potential or by changed channel kinetics. A change in the reversal potential, if occurs, will be probably also reflected in the measured conductance at higher HP compressions. This did not happen. However, a faster TTP was measured at 0.5 MPa (see below section), suggesting a mechanism through which elevated total ionic flux could develop without an increase in the steady-state conductance.

Decompression was successful in the $Ca_V2.2_{+\gamma2}$, but only partially recovered conductance in $Ca_V2.2$, which was still slightly augmented. Should the conductance remain high for long duration after decompression (presently not tested) in the living organism, that may lead to excitotoxicity of neurons due to high cytosolic [Ca^{2+}], which could explain the long-term cognitive deficits found in veteran occupational deep divers [61–64].

Currents' TTP and τ_{Rise}

For the $Ca_V2.1$, only a tendency for an elongation of TTP and τ_{Rise} at V_{Imax} at 5.0 MPa was witnessed, whereas in the $Ca_V2.2$, there was a mixed response to HP: At low HP (0.5 MPa), TTP decreased, while at high HP (2.5–5.0 MPa), it tended to increase (Fig. 5D). Interestingly, in the $Ca_V2.2_{+\gamma2}$, both TTP and τ_{Rise} elongate at HP, without recovery after decompression, similarly to the HP effect reported in VDCCs in frog motor nerve (possibly $Ca_V2.2$) [15], guinea pig single cerebellar Purkinje cells (probably $Ca_V2.1$) [17] and in isolated $Ca_V1.2$ expressed in oocytes [30]. The velocity of an action potential was also reduced at HP after a transient increase [16].

Increased measured TTP may also indicate a slower inactivation process, which will make the maximal current appear later. Indeed, the $\tau_{Decay\ Fast}$ was also elongated in $Ca_V2.2_{+\gamma2}$ at HP (Fig. 7F, see Current inactivation). Overall, greater ionic flux *via* $Ca_V2.2_{+\gamma2}$ could be generated per given depolarization at HP, due to increased conductance and maximal currents and deceleration of inactivation kinetics.

Current inactivation

A stronger inactivation in the $Ca_V2.2$ at HP was also supported by shorter $\tau_{Decay\ Fast}$ and $\tau_{Decay\ Slow}$ (Figs 7 and 8). Interestingly, at 5.0 MPa, stronger depolarization (ΔV >20 mV) weakened the inactivation, suggesting the HP effect is also dependent on the currents' driving-force, *i.e.* membrane potential.

Almost no significant effect of HP on inactivation value was measured in the $Ca_V2.1$, excluding some changes at 2.5 MPa but with marginal *p* values, also in $\tau_{Decay\ Slow}$ (Fig. 8). This seems to be a nonlinear HP effect, as was previously found in other VDCCs [30].

In the $Ca_V2.2_{+\gamma2}$, inactivation was weaker at HP throughout the activity range of the channel, which correlated with elongation of both $\tau_{Decay\ Fast}$ and $\tau_{Decay\ Slow}$ (Fig. 4). This is an opposite finding to the result in the $Ca_V2.2$, which may suggest that the $\gamma2$ subunit has a role in the inactivation process of the naïve channel and also the sensitivity of the molecular mechanism controlling the voltage-dependent inactivation to HP. Since the $Ca_V2.2_{+\gamma2}$ may represent a more 'native' channel, this result also conforms with the slower inactivation at HP that was reported in Na^+ channel in bovine chromaffin cells [13]. The effect of HP on both τ_{Decay}s was only at pressures above 0.5 MPa, which is in agreement with the fact that at least 1.0 MPa is needed in order for the HPNS to develop in humans.

Although generally $\tau_{Decay\ Fast}$ and $\tau_{Decay\ Slow}$ were affected similarly by HP for each channel separately (Table 2), both in $Ca_V2.2$ and $Ca_V2.2_{+\gamma2}$, $\tau_{Decay\ Slow}$ was affected differentially than $\tau_{Decay\ Fast}$ at HP for membrane potentials below V_{Imax} (ΔV <0 mV). This further supports the well-established concept of different mechanisms for the fast and slow inactivation [65, 66], which can also react differently to external treatment [67]. It was also demonstrated that the molecular structures responsible for these two types of inactivation are differently located in the VDCC's protein [68] and that the fast inactivation may act similarly to the 'ball and chain' mechanism in the K^+ channel [69], while the slow inactivation seems to be at least partially dependent on the interaction between α_1 and β subunits [66]. As the γ_2 subunit is known to affect these mechanisms [37, 70] and to interact with $Ca_V\beta_3$ subunit, both involved in the channels' modulation by $G\beta\gamma$ [38, 71], it is not surprising that the HP effect on inactivation is altered by the presence or absence of γ_2. The lack of inactivation recovery to control values after decompression in the $Ca_V2.2_{+\gamma2}$ suggests that either the conformational changes related to inactivation that γ_2 is involved in or the interaction site of γ_2 had been irreversibly altered by HP.

It should be noted that even in the absence of Ca^{2+}, still two components of time constants were necessary in order to fit the voltage- and time-dependent inactivating portion of the current. This leads to the notion that the $\tau_{Decay\ Slow}$ described here is also voltage dependent that is usually masked by the relatively faster Ca^{2+}-dependent slow inactivation.

Currents deactivation

All channels examined responded to HP by elongation of τ_{Tail}, whether significantly ($Ca_V2.2$ and $Ca_V2.2_{+\gamma2}$) or just by a tendency ($Ca_V2.1$), implying a slower deactivation at HP (Fig. 9) for these neuronal channels, in oppose to the $Ca_V1.2$ [30]. τ_{Tail} is the only kinetic parameter that was similarly affected in $Ca_V2.2$ and $Ca_V2.2_{+\gamma2}$ channels, suggesting that the γ_2 subunit is not involved in the regulation of the deactivation mechanism.

Overall, this fits well with the general pressure effect on the $Ca_V2.2$ and $Ca_V2.2_{+\gamma2}$ channels witnessed here – an increased flux at HP.

Activation volume ($\Delta V^{\ddagger}$)

Excluding $\tau_{Decay\ Slow}$, all $\Delta V^{\ddagger}$ of $Ca_V2.1$ are 12–29% of $Ca_V2.2$ $\Delta V^{\ddagger}$ values. This conforms with the weaker, or even non-existent, sensitivity of the channel to HP.

All $\Delta V^{\ddagger}$ of τ_{Tail} are positive values, indicating a deceleration by HP. This suggests that the deactivation process is similar in the examined channels, although less sensitive in $Ca_V2.1$, as mentioned above. Interestingly, τ_{Tail} $\Delta V^{\ddagger}$ of $Ca_V1.2$ is negative as reported in our recent study [30], suggesting its deactivation mechanism may operate in a different spatial manner.

All $\Delta V^{\ddagger}$ of $Ca_V2.2_{+\gamma2}$ are positive values, as opposed to the negative τ_{Decay}s $\Delta V^{\ddagger}$ in $Ca_V2.1$, $Ca_V2.2$ and even in $Ca_V1.2$ and $Ca_V3.2$ as also reported in our previous study [30]. This indicates that γ_2 participates in regulation of the inactivation process, a fact that has been revealed by HP exposure.

Summary

HP hardly affected the behaviour of $Ca_V2.1$, but had a major effect in both $Ca_V2.2$ and $Ca_V2.2_{+\gamma2}$, albeit HP kinetic effect was generally opposite in all aspects but τ_{Tail}. These effects may indicate that the conformational changes involved in the channels' activity are facilitated (*e.g.* conductance, $\tau_{Decay\ fast}$ and $\tau_{Decay\ Slow}$ in $Ca_V2.2$) or opposed (*e.g.* inactivation and deactivation in the $Ca_V2.2_{+\gamma2}$) by an elevated ambient pressure. Indeed, this notion is supported by the calculated activation volumes corresponding to these processes, probably affecting the total ionic flux through the channels at HP.

Some of the effects may indicate a transient or non-linear nature (*e.g.* TTP and inactivation in $Ca_V2.2$, respectively), while other suggested that the HP effect may be reversed by decompression (*e.g.* inactivation, TTP, τ_{Rise}, $\tau_{Decay\ Fast}$, $\tau_{Decay\ Slow}$ in the $Ca_V2.2$ and τ_{Tail} in $Ca_V2.1$, but not TTP and τ_{Rise} in $Ca_V2.2_{+\gamma2}$). A qualitative summary of the major HP-induced findings is given in Table 2. Among these effects, some were dependent on the membrane potential (*e.g.* inactivation in $Ca_V2.2$, τ_{Tail} in $Ca_V2.1$) or fluctuated at different HP (*e.g.* TTP and τ_{Rise} in $Ca_V2.2$).

General consideration

Although currents in this study were carried by Ba^{2+} ions (and not Ca^{2+}, due to the reasons detailed in Materials and methods), we believe that regarding the main aspect of interest in HP influence on VDCC, *i.e.* conductance and amplitude of currents, the HP impact on these parameters reflects the modulation of HP when Ca^{2+} ions are moving through the channels' pore, as was clearly demonstrated in our previous study [30]. This, however, does not exclude the possibility that HP may additionally affect Ca^{2+}-dependent mechanisms such as Ca^{2+}-dependent inactivation.

The fact that HP effect was not always consistent in all membrane potentials suggests that one of the pressure targets is the S4 segment in the transmembrane region of α_1, holding the positively charged amino acids sequence that serve as a voltage sensor, thus affecting any voltage-dependent mechanisms, *e.g.* activation and inactivation. Hyperbaric pressure interfering with the spatial movement of S4 segment would also cause a change in the gating current. It was indeed demonstrated in the past that a considerable fraction of $\Delta V^{\ddagger}$ in activation of Na^+ channel is associated with gating current [13, 72].

The non-linear HP effect is reminiscent of a bell-shaped dose–response curve; a certain pressure causes a maximal effect, while lower or higher pressures weaken it. The TTP and τ_{Rise}, that share this behaviour in the $Ca_V2.2$, are different parameters for measuring the channels' activation, which is dependent on membrane potential and the successful spatial transformation of the same S4 segment. This transformation requires a strong enough electrical field to cross a certain energetic threshold. It seems that HP influences that threshold in a non-linear manner (bell-shaped), suggesting the spatial reorganization to be more complex than one hinge or happening on a single plateau.

Undoubtedly, the changes in both magnitude and kinetics of the response to depolarization at HP would influence these channels' functionality in the living organism, and hence also its motor and cognitive performance. Indeed, the HPNS constellation of sign and symptoms includes changes in EEG, sleep disorders, decrements in locomotor activity, myoclonus and tremors, which may all be expressed as the manifestation of these HP-induced changes in VDCCs.

We have previously postulated that even a 'minor' change made to a section within a subunit [73, 74] or just a single amino acid substitution [75, 76] can significantly alter the VDCC reaction to depolarization, possibly due to a different spatial organization [65], let alone the use of different subunits will have this effect. Naturally, this assumption is supported in the first place by the differential response to HP in the $Ca_V2.1$ and $Ca_V2.2$, having a different α_1 subunit comprising the pore and voltage sensor. But further support to this notion is also provided by the differential HP effects in the $Ca_V2.2$ and $Ca_V2.2_{+\gamma2}$. The saturation of current augmentation at 0.5–5.0 MPa in the $Ca_V2.2_{+\gamma2}$ *versus* the dose–response curve of the $Ca_V2.2$ may suggest that the γ subunit counteracts the HP effect on the channels' conductance.

We have recently demonstrated HP effects in VDCC [30] and rat-cultured cortical neurons (unpublished data) already at 0.5 and 0.3 MPa, respectively. Dean & Mulkey (2003) have also reported reversible changes in membrane properties in rat medulla solitary complex upon helium compression to as low as 0.3 MPa. Relatively low HP threshold, 0.5 MPa, was also found here in the $Ca_V2.2$ and $Ca_V2.2_{+\gamma2}$.

Journal of Cellular and Molecular Medicine published by John Wiley & Sons Ltd and Foundation for Cellular and Molecular Medicine.

Since HP can target either the channel (and its subunits) or any external modulator, and although the general impression from this study is that HP affects the channel itself by changing its spatial organization in the active or non-active states, further research is needed to determine whether VDCCs' modulators are also affected by HP. Notwithstanding, ion channel configuration may also be affected by the membrane characteristics (*e.g.* fluidity, input resistance, specific capacity), which have been shown to be affected by HP [55, 77–79], even at low HP as well (<0.4 MPa) [80]. Barosensitivity is commonly attributed to be a manifestation of pressure equally exerted in all dimensions, whereas mechanosensitivity is caused by localized shear and strain forces manifested (at HP) by differences in compressibility of adjacent cellular structures [81, 82]. Mechanosensitivity of biological processes has been also demonstrated at relatively low HP (<0.2 MPa) [83], as opposed to barosensitivity of the channel, which usually occurs at high HP (>0.5 and up to 10–40 MPa) [13, 17]. This notion may provide another explanation for the non-linear HP effect: low HP affected the channel *via* altered membrane traits and perhaps mechanosensitivity, while high HP affected the channels itself as well.

On the other hand, a direct influence of HP on the channel may be supported by crystallographic work that has shown the presence of a hydrophobic cavity within a protein, the ability of gas molecules to penetrate it and a reduction in its volume at HP [84, 85]. Such a cavity has been proposed to have a role in protein flexibility, which in turn is related to functional efficiency [86]. Hence, should a VDCC contain such a cavity, changes in its volume or presence or lack of a gas molecule in it could have a crucial HP-induced influence on the protein functionality. Such a distortion in the spatial organization and/or conformational change of the channel will also undoubtedly interfere with a prompt recovery back to its naïve state and may provide an explanation for the lack of complete recovery of the channel after decompression in general, and specifically within the time frame of our experiments.

Overall, the direct data being accumulated regarding HP-induced effects in several types of VDCCs thus far strongly suggest that the previous concept of uniform influence of HP on certain types of channels should be abandoned. As demonstrated by our group, pressure may augment or depress currents, accelerate or decelerate kinetics or leave some of the channels' traits unaffected. The actual mechanism (s) underlying this diversity of responses to HP need further elucidation. Yet, we may speculate that the wide spectrum of pressure sensitivity in vertebrates (*e.g.* tolerance to various levels of HP, while others are obligatory high HP dwellers) is, at least in part, the result of evolutionary differential distribution of these VDCCs throughout neuronal networks, along the single neuron, or structural variations of the same channel in different life forms.

Conclusions

a. HP-selective modulation of various presynaptic VDCCs (in addition to somatic and dendritic channels) probably has an important role in synaptic transmission alteration, which is strongly associated with HPNS.
b. HP selectivity depends on the different α_1 subunit comprising the pore and voltage sensor but can also be mediated by other regulatory subunits of the channel protein.
c. Pressure modulation of channels' kinetics and function is dependent on the membrane potential.

Acknowledgements

This work was supported by USA ONR grant no. N00014-10-1-0163 to Y. Grossman. We thank Prof. N. Dascal from the Department of Physiology and Pharmacology, Sackler School of Medicine, Tel Aviv University, for donating $Ca_V2.2$ subunits cRNA, and Prof. D. Atlas from the Department of Biological Chemistry, The Silverman Institute of Life Sciences, The Hebrew University of Jerusalem, for donating $Ca_V2.1$ subunits cRNA.

Conflict of interest

The authors confirm that there are no conflicts of interest.

References

1. **Daniels S, Grossman Y.** Pressure effects on cells. In: Sebert P, editor. *Comparative high pressure biology*. Enfield, New Hampshire: Science Publishers; 2010. pp. 121–42.
2. **Bennett PB.** Inert gas narcosis and high pressure nervous syndrome. *Bove and Davis' Diving Medicine*. 1997; 3: 117–30.
3. **Abraini JH.** Inert gas and raised pressure: evidence that motor decrements are due to pressure per se and cognitive decrements due to narcotic action. *Pflugers Arch*. 1997; 433: 788–91.
4. **Tarasiuk A, Grossman Y.** Pressure-induced tremor-associated activity in ventral roots in isolated spinal cord of newborn rats. *Undersea Biomed Res*. 1990; 17: 287–96.
5. **Darbin O, Risso JJ, Rostain JC.** High pressure enhanced NMDA activity in the striatum and the globus pallidus: relationships with myoclonia and locomotor and motor activity in rat. *Brain Res*. 2000; 852: 62–7.
6. **Logue PE, Schmitt FA, Rogers HE, *et al.*** Cognitive and emotional changes during a simulated 686-m deep dive. *Undersea Biomed Res*. 1986; 13: 225–35.
7. **Overman WH, Brauer RW, Burke ER.** Failure to find residual memory deficits in monkeys after repeated HPNS. *Undersea Biomed Res*. 1989; 16: 115–27.
8. **Steevens CC, Russell KL, Knafelc ME, *et al.*** Noise-induced neurologic disturbances in divers exposed to intense water-borne sound: two case reports. *Undersea Hyperb Med*. 1999; 26: 261–5.
9. **Vaernes RJ, Bergan T, Warncke M.** HPNS effects among 18 divers during compression to 360 msw on heliox. *Undersea Biomed Res*. 1988; 15: 241–55.
10. **Rostain JC, Gardette-Chauffour MC, Naquet R.** EEG and sleep disturbances during dives at 450 msw in helium-nitrogen-oxygen mixture. *J Appl Physiol*. 1997; 83: 575–82.
11. **Bennett PB, Rostain C.** High pressure nervous syndrome. In: Brubakk AO, Neuman

TS, editors. *Bennett and Elliott's physiology and medicine of diving*. Edinburgh: W.B. Saunders; 2003. pp. 323–57.

12. **Grossman Y, Aviner B, Mor A.** High pressure effects on mammalian central nervous system. In: Sebert P, editor. *Comparative high pressure biology*. Enfield, New Hampshire: Science Publishers; 2010. pp. 161–86.
13. **Heinemann SH, Conti F, Stuhmer W, *et al.*** Effects of hydrostatic pressure on membrane processes. Sodium channels, calcium channels, and exocytosis. *J Gen Physiol*. 1987; 90: 765–78.
14. **Shelton CJ, Doyle MG, Price DJ, *et al.*** The effect of high pressure on glycine- and kainate-sensitive receptor channels expressed in Xenopus oocytes. *Proc Biol Sci*. 1993; 254: 131–7.
15. **Aviner B, Gradwohl G, Moore HJ, *et al.*** Modulation of presynaptic Ca^{2+} currents in frog motor nerve terminals by high pressure. *Eur J Neurosci*. 2013; 38: 2716–29.
16. **Grossman Y, Kendig JJ.** Pressure and temperature modulation of conduction in a bifurcating axon. *Undersea Biomed Res*. 1986; 13: 45–61.
17. **Etzion Y, Grossman Y.** Spontaneous Na^{+} and Ca^{2+} spike firing of cerebellar Purkinje neurons at high pressure. *Pflugers Arch*. 1999; 437: 276–84.
18. **Parmentier JL, Shrivastav BB, Bennett PB.** Hydrostatic pressure reduces synaptic efficiency by inhibiting transmitter release. *Undersea Biomed Res*. 1981; 8: 175–83.
19. **Ashford ML, MacDonald AG, Wann KT.** The effects of hydrostatic pressure on the spontaneous release of transmitter at the frog neuromuscular junction. *J Physiol*. 1982; 333: 531–43.
20. **Etzion Y, Mor A, Grossman Y.** Differential modulation of cerebellar climbing fiber and parallel fiber synaptic responses at high pressure. *J Appl Physiol*. 2008; 2008: 90853.
21. **Gilman SC, Colton JS, Dutka AJ.** Effect of pressure on the release of radioactive glycine and gamma-aminobutyric acid from spinal cord synaptosomes. *J Neurochem*. 1987; 49: 1571–8.
22. **Golan H, Colton JS, Moore HJ, *et al.*** Analysis of evoked and spontaneous quantal release at high pressure in crustacean excitatory synapses. *Pflugers Arch*. 1995; 430: 617–25.
23. **Golan H, Moore HJ, Grossman Y.** Quantal analysis of presynaptic inhibition, low $[Ca^{2+}]$ 0, and high pressure interactions at crustacean excitatory synapses. *Synapse*. 1994; 18: 328–36.
24. **Golan H, Moore HJ, Grossman Y.** Pressure exposure unmasks differences in release properties between high and low yield excitatory synapses of a single crustacean axon. *Neuropharmacology*. 1996; 35: 187–93.
25. **Golan H, Grossman Y.** Synaptic transmission at high pressure: effects of $[Ca^{2+}]$o. *Comp Biochem Physiol Comp Physiol*. 1992; 103: 113–8.
26. **Grossman Y, Kendig JJ.** Synaptic integrative properties at hyperbaric pressure. *J Neurophysiol*. 1988; 60: 1497–512.
27. **Grossman Y, Kendig JJ.** Evidence for reduced presynaptic Ca^{2+} entry in a lobster neuromuscular junction at high pressure. *J Physiol*. 1990; 420: 355–64.
28. **Talpalar AE, Giugliano M, Grossman Y.** Enduring medial perforant path short-term synaptic depression at high pressure. *Front Cell Neurosci*. 2010; 4: 128.
29. **Talpalar AE, Grossman Y.** Modulation of rat corticohippocampal synaptic activity by high pressure and extracellular calcium: single and frequency responses. *J Neurophysiol*. 2003; 90: 2106–14.
30. **Aviner B, Gradwohl G, Mor Aviner M, *et al.*** Selective modulation of cellular voltage dependent calcium channels by hyperbaric pressure - a suggested HPNS partial mechanism. *Front Cell Neurosci*. 2014; 8: 136. doi: 10.3389/fncel.2014.00136
31. **Meir A, Ginsburg S, Butkevich A, *et al.*** Ion channels in presynaptic nerve terminals and control of transmitter release. *Physiol Rev*. 1999; 79: 1019–88.
32. **Catterall WA.** Structure and regulation of voltage-gated Ca^{2+} channels. *Annu Rev Cell Dev Biol*. 2000; 16: 521–55.
33. **Catterall WA.** Structure and function of voltage-gated ion channels. *Annu Rev Biochem*. 1995; 64: 493–531.
34. **Varadi G, Mori Y, Mikala G, *et al.*** Molecular determinants of Ca^{2+} channel function and drug action. *Trends Pharmacol Sci*. 1995; 16: 43–9.
35. **Hofmann F, Biel M, Flockerzi V.** Molecular basis for Ca^{2+} channel diversity. *Annu Rev Neurosci*. 1994; 17: 399–418.
36. **Hosey MM, Chien AJ, Puri TS.** Structure and regulation of L-type calcium channels a current assessment of the properties and roles of channel subunits. *Trends Cardiovasc Med*. 1996; 6: 265–73.
37. **Letts VA, Felix R, Biddlecome GH, *et al.*** The mouse stargazer gene encodes a neuronal Ca^{2+}-channel gamma subunit. *Nat Genet*. 1998; 19: 340–7.
38. **Tselnicker I, Tsemakhovich VA, Dessauer CW, *et al.*** Stargazin modulates neuronal voltage-dependent Ca^{2+} channel Cav2.2 by a G{beta}{gamma}-dependent mechanism. *J Biol Chem*. 2010; 285: 20462–71.
39. **Aviner B, Gnatek Y, Gradwohl G, *et al.*** Hyperbaric pressure effects on voltage-dependent Ca+2 channels: relevance to HPNS. *Undersea Hyperb Med*. 2010; 37: 245–58.
40. **Grossman Y, Colton JS, Gilman SC.** Interaction of Ca-channel blockers and high pressure at the crustacean neuromuscular junction. *Neurosci Lett*. 1991; 125: 53–6.
41. **Etzion Y, Grossman Y.** Pressure-induced depression of synaptic transmission in the cerebellar parallel fibre synapse involves suppression of presynaptic N-type Ca^{2+} channels. *Eur J Neurosci*. 2000; 12: 4007–16.
42. **Otter T, Salmon ED.** Pressure-induced changes in Ca^{2+}-channel excitability in Paramecium. *J Exp Biol*. 1985; 117: 29–43.
43. **Heidelberger R, Zhou Z-Y, Matthews G.** Multiple components of membrane retrieval in synaptic terminals revealed by changes in hydrostatic pressure. *J Neurophysiol*. 2002; 88: 2509–17.
44. **Gilman SC, Colton JS, Dutka AJ, *et al.*** Effects of high pressure on the release of excitatory amino acids by brain synaptosomes. *Undersea Biomed Res*. 1986; 13: 397–406.
45. **Miledi R, Parker I.** Chloride current induced by injection of calcium into Xenopus oocytes. *J Physiol*. 1984; 357: 173–83.
46. **Catterall WA, Perez-Reyes E, Snutch TP, *et al.*** Nomenclature and structure-function relationships of voltage-gated calcium channels, international union of pharmacology. XLVIII. *Pharmacol Rev*. 2005; 57: 411–25.
47. **Cohen-Kutner M, Nachmanni D, Atlas D.** CaV2.1 (P/Q channel) interaction with synaptic proteins is essential for depolarization-evoked release. *Channels (Austin)*. 2010; 4: 266–77.
48. **Kendig J, Grossman Y, Heinemann SH.** Ion channels and nerve cell function. In: Macdonald AG, editor. *Advances in comparative and environmental physiology, effects of high pressure on biological systems*. Berlin-Heidelberg: Springer-Verlag; 1993. pp. 88–124.
49. **Dean JB, Mulkey DK, Garcia AJ III, *et al.*** Neuronal sensitivity to hyperoxia, hypercapnia, and inert gases at hyperbaric pressures. *J Appl Physiol*. 2003; 95: 883–909.
50. **Andronache Z, Ursu D, Lehnert S, *et al.*** The auxiliary subunit {gamma}1 of the skeletal muscle L-type Ca^{2+} channel is an endogenous Ca^{2+} antagonist. *PNAS*. 2007; 104: 17885–90.
51. **Henderson JV, Gilbert DL.** Slowing of ionic currents in the voltage-clamped squid axon by helium pressure. *Nature*. 1975; 258: 351–2.

Journal of Cellular and Molecular Medicine published by John Wiley & Sons Ltd and Foundation for Cellular and Molecular Medicine.

52. **Conti F, Fioravanti R, Segal JR, *et al.*** Pressure dependence of the potassium currents of squid giant axon. *J Membr Biol*. 1982; 69: 35–40.
53. **Shrivastav BB PJ, Bennett PB.** A Quantitative description of pressure-induced alterations in ionic channels of the squid giant axon. Seventh Symposium on Underwater Physiology, Undersea Society Inc. 1981; 7: 611–9.
54. **Harper AA, Macdonald AG, Wann KT.** The action of high hydrostatic pressure on the membrane currents of Helix neurones. *J Physiol*. 1981; 311: 325–39.
55. **Grossman Y, Kendig JJ.** Pressure and temperature: time-dependent modulation of membrane properties in a bifurcating axon. *J Neurophysiol*. 1984; 52: 693–708.
56. **Uchitel OD, Protti DA, Sanchez V, *et al.*** P-type voltage-dependent calcium channel mediates presynaptic calcium influx and transmitter release in mammalian synapses. *PNAS*. 1992; 89: 3330–3.
57. **Wheeler DB, Randall A, Tsien RW.** Roles of N-type and Q-type Ca^{2+} channels in supporting hippocampal synaptic transmission. *Science*. 1994; 264: 107–11.
58. **Mintz IM, Sabatini BL, Regehr WG.** Calcium control of transmitter release at a cerebellar synapse. *Neuron*. 1995; 15: 675–88.
59. **Westenbroek RE, Hell JW, Warner C, *et al.*** Biochemical properties and subcellular distribution of an N-type calcium channel alpha 1 subunit. *Neuron*. 1992; 9: 1099–115.
60. **Talpalar AE, Grossman Y.** Enhanced excitability compensates for high-pressure-induced depression of cortical inputs to the hippocampus. *J Neurophysiol*. 2004; 92: 3309–19.
61. **Leplow B, Tetzlaff K, Holl D, *et al.*** Spatial orientation in construction divers–are there associations with diving experience? *Int Arch Occup Environ Health*. 2001; 74: 189–98.
62. **Calder I.** Does diving damage your brain? *Occup Med*. 1992; 42: 213–4.
63. **Todnem K, Nyland H, Skeidsvoll H, *et al.*** Neurological long term consequences of deep diving. *Occup Environ Med*. 1991; 48: 258–66.
64. **Vaernes RJ, Klove H, Ellertsen B.** Neuropsychologic effects of saturation diving. *Undersea Biomed Res*. 1989; 16: 233–51.
65. **Hering S, Berjukow S, Sokolov S, *et al.*** Molecular determinants of inactivation in voltage-gated Ca^{2+} channels. *J Physiol*. 2000; 528: 237–49.
66. **Sokolov S, Weiss RG, Timin EN, *et al.*** Modulation of slow inactivation in class A Ca^{2+} channels by {beta}-subunits. *J Physiol*. 2000; 527: 445–54.
67. **Livneh A, Cohen R, Atlas D.** A novel molecular inactivation determinant of voltage-gated CaV1.2 L-type Ca^{2+} channel. *Neuroscience*. 2006; 139: 1275–87.
68. **Berjukow S, Gapp F, Aczel S, *et al.*** Sequence differences between alpha 1C and alpha 1S Ca^{2+} channel subunits reveal structural determinants of a guarded and modulated benzothiazepine receptor. *J Biol Chem*. 1999; 274: 6154–60.
69. **Cens T, Restituito S, Galas S, *et al.*** Voltage and calcium use the same molecular determinants to inactivate calcium channels. *J Biol Chem*. 1999; 274: 5483–90.
70. **Klugbauer N, Dai S, Specht V, *et al.*** A family of gamma-like calcium channel subunits. *FEBS Lett*. 2000; 470: 189–97.
71. **Zhang Y, Chen Y-h, Bangaru SD, *et al.*** Origin of the voltage dependence of G-protein regulation of P/Q-type Ca^{2+} channels. *J Neurosci*. 2008; 28: 14176–88.
72. **Conti F, Inoue I, Kukita F, *et al.*** Pressure dependence of sodium gating currents in the squid giant axon. *Eur Biophys J*. 1984; 11: 137–47.
73. **Zhang JF, Ellinor PT, Aldrich RW, *et al.*** Molecular determinants of voltage-dependent inactivation in calcium channels. *Nature*. 1994; 372: 97–100.
74. **Tang S, Yatani A, Bahinski A, *et al.*** Molecular localization of regions in the L-type calcium channel critical for dihydropyridine action. *Neuron*. 1993; 11: 1013–21.
75. **Hans M, Urrutia A, Deal C, *et al.*** Structural elements in domain IV that influence biophysical and pharmacological properties of human alpha1A-containing high-voltage-activated calcium channels. *Biophys J* . 1999; 76: 1384–400.
76. **Bourinet E, Soong TW, Sutton K, *et al.*** Splicing of alpha 1A subunit gene generates phenotypic variants of P- and Q-type calcium channels. *Nat Neurosci*. 1999; 2: 407–15.
77. **Benz R, Conti F.** Effects of hydrostatic pressure on lipid bilayer membranes. I. Influence on membrane thickness and activation volumes of lipophilic ion transport. *Biophys J* . 1986; 50: 91–8.
78. **Moskovitz Y, Yang H.** Modelling of noble anaesthetic gases and high hydrostatic pressure effects in lipid bilayers. *Soft Matter*. 2015; 11: 2125–38.
79. **Macdonald AG, Wahle KW, Cossins AR, *et al.*** Temperature, pressure and cholesterol effects on bilayer fluidity; a comparison of pyrene excimer/monomer ratios with the steady-state fluorescence polarization of diphenylhexatriene in liposomes and microsomes. *Biochim Biophys Acta*. 1988; 938: 231–42.
80. **Mulkey DK, Henderson RA III, Putnam RW, *et al.*** Pressure (<4 ATA) increases membrane conductance and firing rate in the rat solitary complex. *J Appl Physiol*. 2003; 95: 922–30.
81. **Macdonald AG.** Hydrostatic pressure as an environmental factor in life processes. *Comp Biochem Physiol Part A Physiol*. 1997; 116: 291–7.
82. **Macdonald AG, Fraser PJ.** The transduction of very small hydrostatic pressures. *Comp Biochem Physiol Part A Mol Integr Physiol*. 1999; 122: 13–36.
83. **Fraser PJ, Macdonald AG.** Crab hydrostatic pressure sensors. *Nature*. 1994; 371: 383.
84. **Marassio G, Prange T, David HN, *et al.*** Pressure-response analysis of anesthetic gases xenon and nitrous oxide on urate oxidase: a crystallographic study. *FASEB J*. 2011; 25: 2266–75.
85. **Girard E, Marchal S, Perez J, *et al.*** Structure-function perturbation and dissociation of tetrameric urate oxidase by high hydrostatic pressure. *Biophys J* . 2010; 98: 2365–73.
86. **Hubbard SJ, Argos P.** A functional role for protein cavities in domain: domain motions. *J Mol Biol*. 1996; 261: 289–300.